

Technical Report No. 32-188

Fission-Fragment Energy Loss
From Vortex Tubes

Henry J. Stumpf



JET PROPULSION LABORATORY
CALIFORNIA INSTITUTE OF TECHNOLOGY
PASADENA, CALIFORNIA

March 12, 1962

**Copyright © 1962
Jet Propulsion Laboratory
California Institute of Technology**

CONTENTS

I. Introduction	1
II. Assumptions	2
III. Analysis	3
IV. Results	7
V. Conclusions	12
Nomenclature	12

FIGURES

1. Cylindrical-coordinate system	3
2. Regions of integration: $\lambda_1 < 2R$	4
3. Regions of integration: $\lambda_1 > 2R$	4
4. Fraction of fission-fragment energy lost from vortex tube as a function of k_1 linear energy	5
5. Fraction of fission-fragment energy lost from vortex tube as a function of linear velocity	5
6. Fraction of total fission-fragment energy lost from vortex tube as a function of vortex-tube diameter; linear velocity	8
7. Fraction of total fission-fragment energy lost from vortex tube as a function of vortex-tube diameter; linear velocity, $W = 0.2$	8
8. Fraction of total fission-fragment energy lost from vortex tube as a function of vortex-tube diameter; linear energy, $W = 0.5$	9
9. Fraction of total fission-fragment energy lost from vortex tube as a function of vortex-tube diameter; linear velocity, $W = 0.5$	10
10. Fraction of total fission-fragment energy lost from vortex tube as a function of vortex-tube diameter; linear energy, $W = 1.0$	10
11. Fraction of total fission-fragment energy lost from vortex tube as a function of vortex-tube diameter; linear velocity, $W = 1.0$	11

ABSTRACT

The heat load in the solid regions of the vortex-tube reactor due to fission fragments reaching the tube walls has been calculated according to a simplified model. Within the limits of the analysis, it can be seen that this heat load is reduced to a few percent of the total power if the diameter of the vortex tubes is greater than 20 cm at an exhaust pressure of 100 atm and greater than 8 cm at 300 atm. As the tube diameter is increased beyond these values, the effect on the fission-fragment heat load is small, and the dependence upon the specific impulse ratio I and the ratio of fuel to propellant density W becomes insignificant.

I. INTRODUCTION

The performance capability of nuclear rockets has been limited to date by the temperature constraints imposed by the structural requirements of the system. Conventional methods of power removal do not allow the full potential of the fission process to be utilized, resulting in reactor operating temperatures, propellant enthalpy gains, and specific impulses which are relatively modest. One means of uncoupling the reactor system from these restraints is to provide a non-temperature-limited or gaseous region of fuel-bearing material. A concept of the gaseous-fuel reactor of particular interest employs vortex containment which allows intimate mixing of the propellant and fissionable species. The gas-phase separation may be accomplished by a system of cylindrical cavities in the reactor core, each of which contains a vortex flow field.

An analysis of laminar, inviscid, two-dimensional vortex flow¹ has shown the mass-flow rate per unit length of vortex tube to be independent of the tube radius, so that high thrust can be obtained by using a large number of vortex tubes. To keep system weight and fuel inventory at reasonable levels, the reactor size and void fraction

must be limited; this implies small-radius tubes. It is not feasible to reduce the radius of the vortex tubes below certain limits, however, because of mechanical design considerations, increased heat load in the solid regions due to gas radiation and fission fragments, and gas-dynamic requirements on propellant mass-flow rate per unit length of vortex tube and nozzle-throat area.

The range of vortex-tube radii determined by the required propellant mass-flow rate for an adequate separation process has been considered in a previous report². It is the purpose of the following analysis to determine the heat load in the solid regions of the reactor core from fission fragments and its dependence upon tube radius and fission-fragment range. It is clear that the fission-fragment heat load will impose a lower limit on the tube radius, since a large fraction of the total fission-fragment energy will be deposited at the walls of the vortex tubes as the tube radius becomes comparable to the fission-fragment range. The other factors which limit the vortex-tube radius will not be considered in this Report.

¹J. L. Kerrebrock and R. V. Meghablian, "Vortex Containment for the Gaseous-Fission Rocket," *Journal of the Aerospace Sciences*, September 1961, pp. 710-724.

²H. J. Stumpf, *Vortex-Tube and Regenerative-Cooling-Tube Parameters for Gaseous-Fission Reactors*, Technical Report No. 32-201, Jet Propulsion Laboratory, Pasadena, Calif., January 22, 1962.

II. ASSUMPTIONS

To avoid mathematical difficulties, it is necessary to consider a simplified model of the vortex tube. In general, the gas in the tube will be a complex mixture of hydrogen, fissionable material, and the multitude of other species arising from the fission process and high temperatures. In addition, the composition, density, and temperature of the mixture will change significantly from the outer wall to the center of the tube, so that any attempt to compute the range of a fission fragment, born at some point in the vortex tube with velocity in a given direction would be exceedingly difficult if not impossible at the present time. Therefore, to make the problem more tractable, it is necessary to consider it on a somewhat macroscopic scale, and the following simplifying assumptions are made:

1. Each fission results in the production of one heavy and one light fission fragment.
2. The fission fragments are released isotropically.
3. The properties of the gaseous mixture in the vortex tube are taken to be those of hydrogen, and appropriate average values are used to correct the ranges

of the light and heavy fission fragments from the values at standard conditions.

4. The length of the vortex tube is large compared to the fission-fragment ranges.
5. The power density in the vortex tube is a known function of the radius.
6. The energy loss of the fission fragments is a known function of the path length.

Assumption 3 may appear rather restrictive. It was included to simplify the computation of the fission-fragment ranges for various pressures, temperatures, and fuel loadings in the vortex tubes, so that an estimate of the fraction of fission-fragment energy deposited in the solid regions of the reactor core could be made without undue computational difficulties. Since the primary purpose of this analysis is to present a relatively simple expression for the fission-fragment energy loss from the vortex tube, given an appropriate value for the fragment range, assumption 3 is not a restriction on the validity of the main results. Equations (16), (17), (18), and (19) in Sect. III would be the same regardless of how the fission-fragment range is computed.

III. ANALYSIS

Consider the coordinate system shown in Fig. 1. The volume element is given by

$$dV = r^2 \cos \chi dr d\chi d\psi \quad (1)$$

The number of fissions per second per unit volume is $\phi(r) \Sigma(r)$, and because of assumption 1 (Sect. II), the number of light or heavy fission fragments produced in dV per second is

$$\phi(r) \Sigma(r) dV = \phi(r) \Sigma(r) r^2 \cos \chi dr d\chi d\psi \quad (2)$$

The solid angle subtended at dV by the area element dA is $(dA \cos \Phi) / r^2$ and using assumption 2, the fraction of the fission fragments produced in dV , with velocities in the direction of dA , is $(dA \cos \Phi) / (4\pi r^2)$. It is easy to show that $\cos \Phi = \cos \chi \cos \psi$; hence, the number of light or heavy fission fragments produced in the volume element dV per second, with velocities in the direction of dA , is

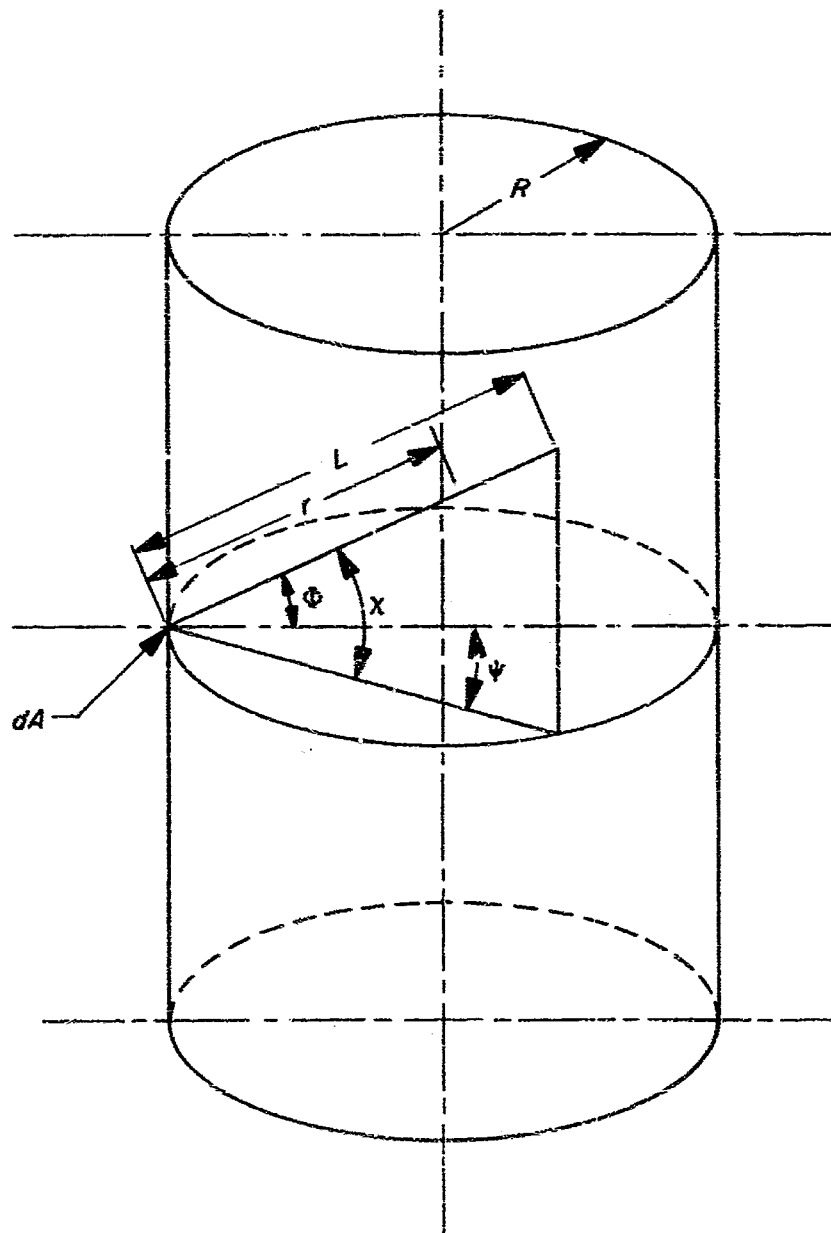


Fig. 1. Cylindrical-coordinate system

$$\frac{1}{4\pi} \phi(r) \Sigma(r) \cos^2 \chi \cos \psi dr d\chi d\psi dA \quad (3)$$

If $E_i(r)$ is the energy of a fission fragment after traversing a distance r , then the rate of energy deposition per unit area at the wall due to fissions in dV is

$$dQ_i = \frac{\phi(r) \Sigma(r) \cos^2 \chi \cos \psi E_i(r)}{4\pi} dr d\chi d\psi \quad (4)$$

where the subscript i refers to the light fragment ($i = L$) or the heavy fragment ($i = H$). Integration of expression (4) over the appropriate volume will yield the rate of energy deposition per unit area of the wall far from the ends of the vortex tube.

It is clear that the limits of integration on the angles ψ and χ are $\pi/2$ to $-\pi/2$. The limits of integration on r , however, are not quite as straightforward to determine. The lower limit is, of course, zero, and the upper limit cannot exceed λ_i , the fission-fragment range. However, there are some values of ψ and χ at which $L < \lambda_i$, in which case the vortex-tube wall defines the bounding surface of the volume of integration. Thus, the upper limit on r is given by either λ_i or L , whichever is the smaller. It is easy to show that

$$L = \frac{2R \cos \psi}{\cos \chi} \quad (5)$$

From Eqs. (4) and (5), the rate of energy deposition per unit area at the wall due to light and heavy fission fragments is

$$Q = \int_V (dQ_L + dQ_H)$$

or

$$Q = \frac{1}{4\pi} \int_{-\pi/2}^{\pi/2} d\psi \int_{-\pi/2}^{\pi/2} d\chi \int_0^{r_L} \phi(r) \Sigma(r) E_L(r) \cos^2 \chi \cos \psi dr \\ + \frac{1}{4\pi} \int_{-\pi/2}^{\pi/2} d\psi \int_{-\pi/2}^{\pi/2} d\chi \int_0^{r_H} \phi(r) \Sigma(r) E_H(r) \cos^2 \chi \cos \psi dr \quad (6)$$

where r_L is the smaller of λ_L and $(2R \cos \psi)/\cos \chi$ and r_H is the smaller of λ_H and $(2R \cos \psi)/\cos \chi$.

It is necessary to distinguish two cases: one in which $\lambda_i < 2R$ and the other in which $\lambda_i > 2R$. In the first instance, there are two regions of integration, as shown in Fig. 2. Region I is a cone-like volume bounded partially by a portion of the base (ABC), partially by rays of length λ_i originating from point A and intersecting the tube wall along the curve BDC, and the shaded curved

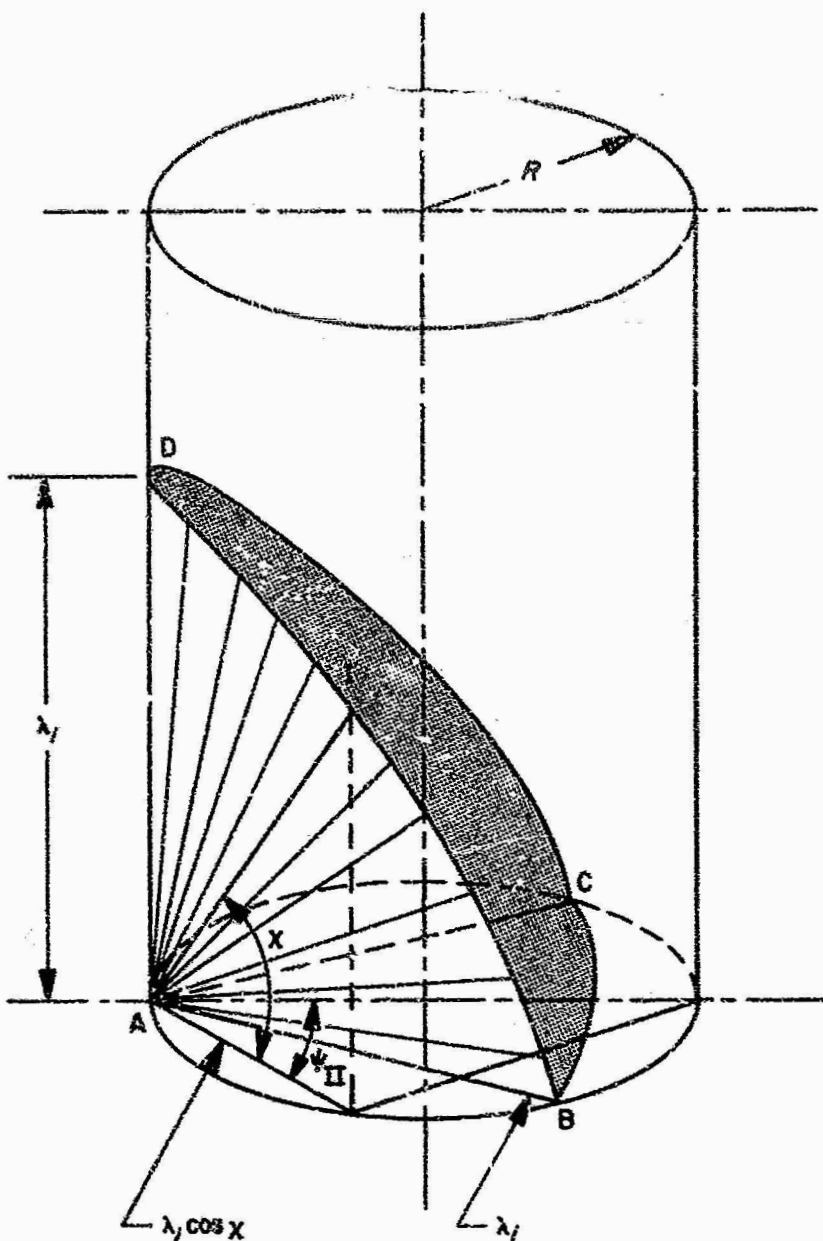


Fig. 2. Regions of integration: $\lambda_i < 2R$

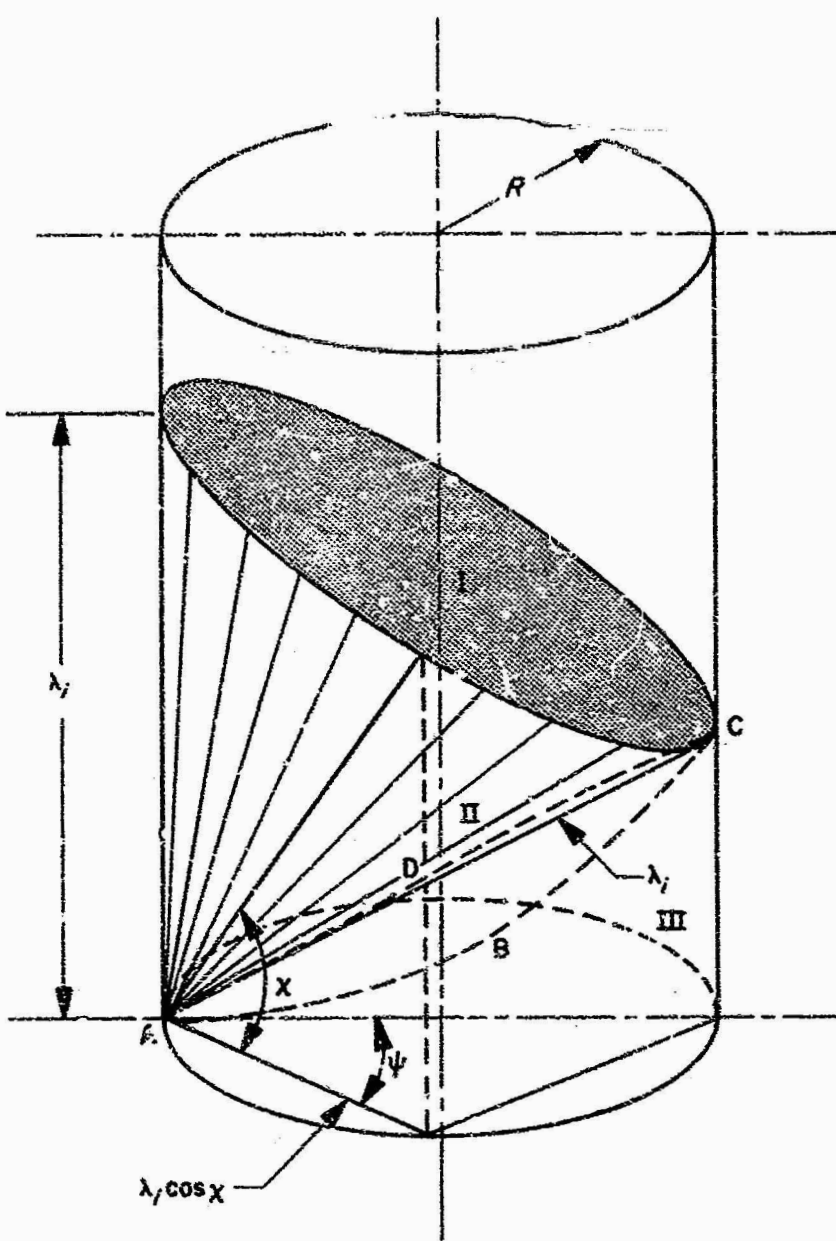


Fig. 3. Regions of integration: $\lambda_i > 2R$

surface. Region II is the remaining volume between the tube wall and Region I, lying below BDC and above the base.

When $\lambda_i > 2R$, three regions of integration must be considered, as shown in Fig. 3. Region I is similar to Region I of the previous case. Region III is the volume bounded by the base, a portion of the tube wall, and a curved surface defined by rays originating from point A at an angle $x = \cos^{-1}(2R / \lambda_i)$ which intersect the tube wall along the line ABCDA. Region II is the volume lying between Regions I and III and bounded by the tube wall.

Below is a summary of the ranges of integrations of the variables for the various regions in each case.

Case I: $\lambda_i < 2R$

Region I

$$0 \leq x \leq \frac{\pi}{2}$$

$$0 \leq \psi \leq \cos^{-1} \frac{\lambda_i \cos x}{2R}$$

$$0 \leq r \leq \lambda_i$$

Region II

$$0 \leq x \leq \frac{\pi}{2}$$

$$\cos^{-1} \frac{\lambda_i \cos x}{2R} \leq \psi \leq \frac{\pi}{2}$$

$$0 \leq r \leq \frac{2R \cos x}{\cos \psi}$$

Case II: $\lambda_i > 2R$

Region I

$$\cos^{-1} \frac{2R}{\lambda_i} \leq x \leq \frac{\pi}{2}$$

$$0 \leq \psi \leq \cos^{-1} \frac{\lambda_i \cos x}{2R}$$

$$0 \leq r \leq \lambda_i$$

Region II

$$\cos^{-1} \frac{2R}{\lambda_i} \leq \chi \leq \frac{\pi}{2}$$

$$\cos^{-1} \frac{\lambda_i \cos \psi}{2R} \leq \psi \leq \frac{\pi}{2}$$

$$0 \leq r \leq \frac{2R \cos \psi}{\cos \chi}$$

Region III

$$0 \leq \chi \leq \cos^{-1} \frac{2R}{\lambda_i}$$

$$0 \leq \psi \leq \frac{\pi}{2}$$

$$0 \leq r \leq \frac{2R \cos \psi}{\cos \chi}$$

The limits in each case are given for one quarter of the total volume, so that the corresponding integrals must be multiplied by a factor of four.

Equation (6) is the expression for the rate of energy deposition per unit area at the tube wall. Multiplying this quantity by the tube-wall area and dividing by the total fission-fragment energy-production rate in the tube will yield the fraction of the fission-fragment energy which is deposited in the solid regions of the reactor core.

Then,

$$\tau = \frac{2\pi Q R l}{E_T \int_V \phi(r) \Sigma(r) dV} \quad (7)$$

and for the case of uniform power production in the tube,

$$\tau = \frac{2\pi Q R l}{E_T \phi \Sigma \pi R^2 l} = \frac{2Q}{\phi \Sigma E_T R} \quad (8)$$

Finally, two expressions for $E_i(r)$ will be considered. In the first, fission-fragment energy is a linear function of distance, so that

$$E_i(r) = E_{0i} \left(1 - \frac{r}{\lambda_i}\right) \quad (9)$$

and in the second, fission-fragment velocity is a linear function of distance, so that

$$E_i(r) = E_{0i} \left(1 - \frac{r}{\lambda_i}\right)^2 \quad (10)$$

Combining the previous equations and considering the case of uniform power production, the following expression for τ results:

$$\tau = a F_L + b F_H \quad (11)$$

where

$$a = \frac{E_L}{2\pi E_T} = 0.09530$$

$$b = \frac{E_H}{2\pi E_T} = 0.09385$$

$$F_i = \frac{4}{R \lambda_i^2} \left[\int_0^{\pi/2} \cos^2 \chi d\chi \int_0^{\cos^{-1} \frac{\lambda_i \cos \chi}{2R}} \cos \psi d\psi \right. \\ \times \int_0^{\lambda_i} (\lambda_i - r)^{\eta} dr + \int_0^{\pi/2} \cos^2 \chi d\chi \\ \times \left. \int_{\cos^{-1} \frac{\lambda_i \cos \chi}{2R}}^{\pi/2} \cos \psi d\psi \int_0^{\frac{2R \cos \psi}{\cos \chi}} (\lambda_i - r)^{\eta} dr \right] \quad (12)$$

when $\lambda_i < 2R$ and

$$F_i = \frac{4}{R \lambda_i^2} \left[\int_{\cos^{-1} \frac{2R}{\lambda_i}}^{\pi/2} \cos^2 \chi d\chi \int_0^{\cos^{-1} \frac{\lambda_i \cos \chi}{2R}} \cos \psi d\psi \right. \\ \times \int_0^{\lambda_i} (\lambda_i - r)^{\eta} dr + \int_{\cos^{-1} \frac{2R}{\lambda_i}}^{\pi/2} \cos^2 \chi d\chi \\ \times \int_{\cos^{-1} \frac{\lambda_i \cos \chi}{2R}}^{\pi/2} \cos \psi d\psi \int_0^{\frac{2R \cos \psi}{\cos \chi}} (\lambda_i - r)^{\eta} dr \\ \left. + \int_0^{\cos^{-1} \frac{2R}{\lambda_i}} \cos^2 \chi d\chi \int_0^{\pi/2} \cos \psi d\psi \right. \\ \times \left. \int_0^{\frac{2R \cos \psi}{\cos \chi}} (\lambda_i - r)^{\eta} dr \right] \quad (13)$$

when $\lambda_i > 2R$. The subscript i may denote the light fragment ($i = L$) or the heavy fragment ($i = H$), and the exponent η denotes which fission-fragment energy law is used (that is, $\eta = 1$ if energy is a linear function of path length and $\eta = 2$ if velocity is a linear function of path length).

The integrals are tedious to evaluate, but it can be done in a fairly straightforward manner. The algebraic details will be omitted and only the results given. The quantities F_i can be shown to depend only upon k , the ratio of the fission-fragment range to the tube diameter; that is,

$$F_i = F_i(k_i) \quad (14)$$

where

$$k_i = \frac{\lambda_i}{2R} \quad (15)$$

In addition, the form of $F_i(k_i)$ changes as the value of k_i changes from less than one to greater than one. The following is a summary of the results of the integrations for the different cases.

Uniform Power: $E_i = E_{oi} [1 - (r/\lambda_i)]$

I. $0 \leq k_i \leq 1$ ($\lambda_i \leq 2R$)

$$F_i(k_i) = \frac{8}{9k_i} \left[(7 + k_i^2) \tilde{E}\left(\frac{\pi}{2}, k_i\right) - 4(1 - k_i^2) \tilde{F}\left(\frac{\pi}{2}, k_i\right) - \frac{3}{2}\pi \right] \quad (16)$$

II. $k_i \geq 1$ ($\lambda_i \geq 2R$)

$$F_i(k_i) = \frac{8}{9} \left[(7 + k_i^2) \tilde{E}\left(\frac{\pi}{2}, \frac{1}{k_i}\right) - (k_i^2 - 1) \left(1 + \frac{3}{k_i^2} \right) \tilde{F}\left(\frac{\pi}{2}, \frac{1}{k_i}\right) - \frac{3\pi}{2k_i} \right] \quad (17)$$

III. Special Cases

a. $F_i(0) = 0$

b. $F_i(1) = \frac{64 - 12\pi}{9} = 2.922$

c. $F_i(\infty) = 2\pi$

Uniform Power: $E_i = E_{oi} [1 - (r/\lambda_i)]^2$

I. $0 \leq k_i \leq 1$ ($\lambda_i \leq 2R$)

$$F_i(k_i) = \frac{1}{9k_i} \left[\frac{9S(k_i)}{k_i} - 24\pi + (73 + 4k_i^2) \tilde{E}\left(\frac{\pi}{2}, k_i\right) - 34(1 - k_i^2) \tilde{F}\left(\frac{\pi}{2}, k_i\right) \right] \quad (18)$$

II. $k_i \geq 1$ ($\lambda_i \geq 2R$)

$$F_i(k_i) = \frac{1}{9} \left[\frac{9G\left(\frac{1}{k_i}\right)}{k_i^2} - \frac{24\pi}{k_i} + \frac{9\pi}{4k_i^2} \ln \frac{k_i + \sqrt{k_i^2 - 1}}{k_i - \sqrt{k_i^2 - 1}} + (73 + 4k_i^2) \tilde{E}\left(\frac{\pi}{2}, \frac{1}{k_i}\right) - (39 + 4k_i^2) \left(1 - \frac{1}{k_i^2} \right) \tilde{F}\left(\frac{\pi}{2}, \frac{1}{k_i}\right) \right] \quad (19)$$

III. Special Cases

a. $F_i(0) = 0$

b. $F_i(1) = \frac{77 - 24\pi}{9} + 1.832 = 2.010$

c. $F_i(\infty) = 2\pi$

The various terms are defined as follows:

$$\tilde{F}\left(\frac{\pi}{2}, \alpha\right) = \int_0^{\pi/2} \frac{d\phi}{\sqrt{1 - \alpha^2 \sin^2 \phi}}$$

(complete elliptic integral of the first kind)

$$\tilde{E}\left(\frac{\pi}{2}, \alpha\right) = \int_0^{\pi/2} \sqrt{1 - \alpha^2 \sin^2 \phi} d\phi$$

(complete elliptic integral of the second kind)

$$S(\beta) = \int_0^{\pi/2} \frac{\sin^{-1}(\beta \cos x)}{\cos x} dx \\ \simeq \frac{\beta\pi}{2} (1 + 0.0833\beta^2 + 0.0281\beta^4 + 0.0139\beta^6 + 0.0083\beta^8 + 0.0055\beta^{10})$$

where $S(1) = 1.832$ and $S(0) = 0.000$.

$$G(\beta) = \int_0^1 \frac{\sin^{-1} \zeta d\zeta}{\zeta \sqrt{1 - \beta^2 \zeta^2}} \\ \simeq (1 + 0.22\beta)(1.0880 + 0.1960\beta^2 + 0.0920\beta^4 + 0.0563\beta^6 + 0.0390\beta^8 + 0.0291\beta^{10})$$

where $G(1) = 1.832$ and $G(0) = (\pi \ln 2)/2 = 1.0830$.

In order to estimate the fraction of the total fission-fragment energy deposited in the solid regions of the reactor, it is necessary to determine the range of the fragments in the vortex tubes. If it is assumed that the range is inversely proportional to the electron concentration, then

$$\rho_s \lambda_s = \rho_i \lambda_i (1 + 0.39 W) \quad (20)$$

where the subscripts s and i refer, respectively, to the properties of hydrogen at standard conditions and in the vortex tube, and the factor $(1 + 0.39 W)$ is the ratio of the electron density in the vortex to that in hydrogen.

For fixed values of I , W , T_p , and P_c and the data given in the article on vortex containment (see footnote 1 on p. 1), the mean propellant density ρ_i and the mean fuel-to-propellant-density ratio W can be determined. The range λ_i can then be computed from Eq. (20).

IV. RESULTS

Equations (16) and (18) are shown in Figs. 4 and 5 for both the light and heavy fission fragments. It can be seen that for values of k_L close to unity (that is, the vortex-tube diameter approximately equal to the range of the light fission fragment) about 45% of the total fission-fragment energy is deposited in the solid regions of the reactor when a linear energy loss is assumed, and about 31% when a linear velocity loss is assumed. These values correspond to 38 and 26%, respectively, of the total fission energy. Since an additional 5 to 10% of the total fission energy is deposited in the solid regions of the reactor as a result of nuclear radiation in the form of neutrons and gamma rays, it is clear that the quantity τ should be minimized.

It would obviously require infinitely large vortex tubes to reduce τ to zero. From Figs. 6 through 11, however, it can be seen that for tube diameters larger than 20 cm at an exhaust pressure of 100 atm and larger than 8 cm at 300 atm, this heat load can be reduced to a few percent of the total power. Further increases in the tube diameter will not decrease the fission-fragment heat load significantly.

It can also be seen from the Figures that, for a fixed set of conditions, the fission-fragment heat load is approximately inversely proportional to the exhaust pressure. At tube diameters at which the fission-fragment heat load is but a few percent of the total power, the specific impulse ratio I and the ratio of fuel to propellant density W have little influence on this heat load.

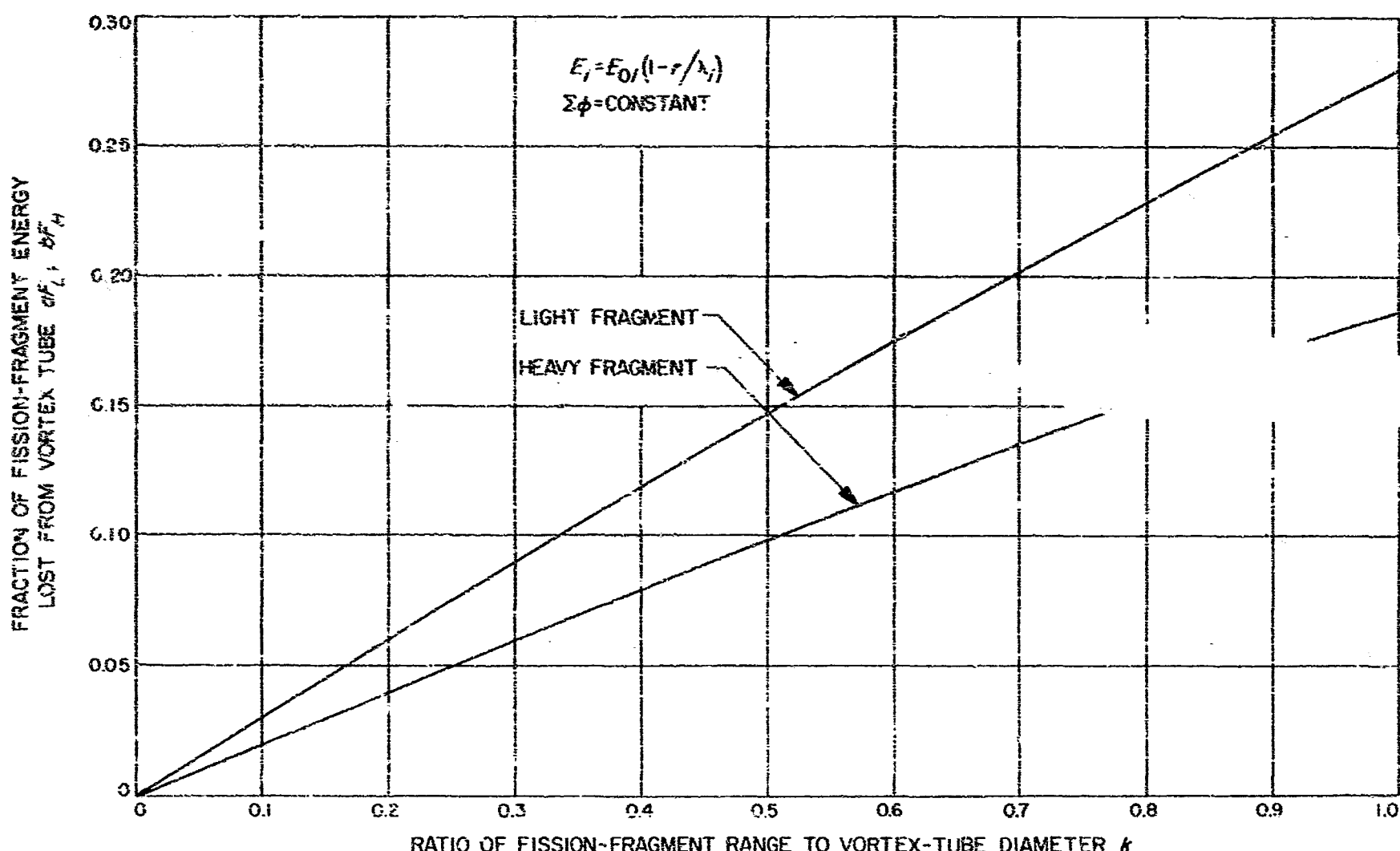


Fig. 4. Fraction of fission-fragment energy lost from vortex tube as a function of k ; linear energy

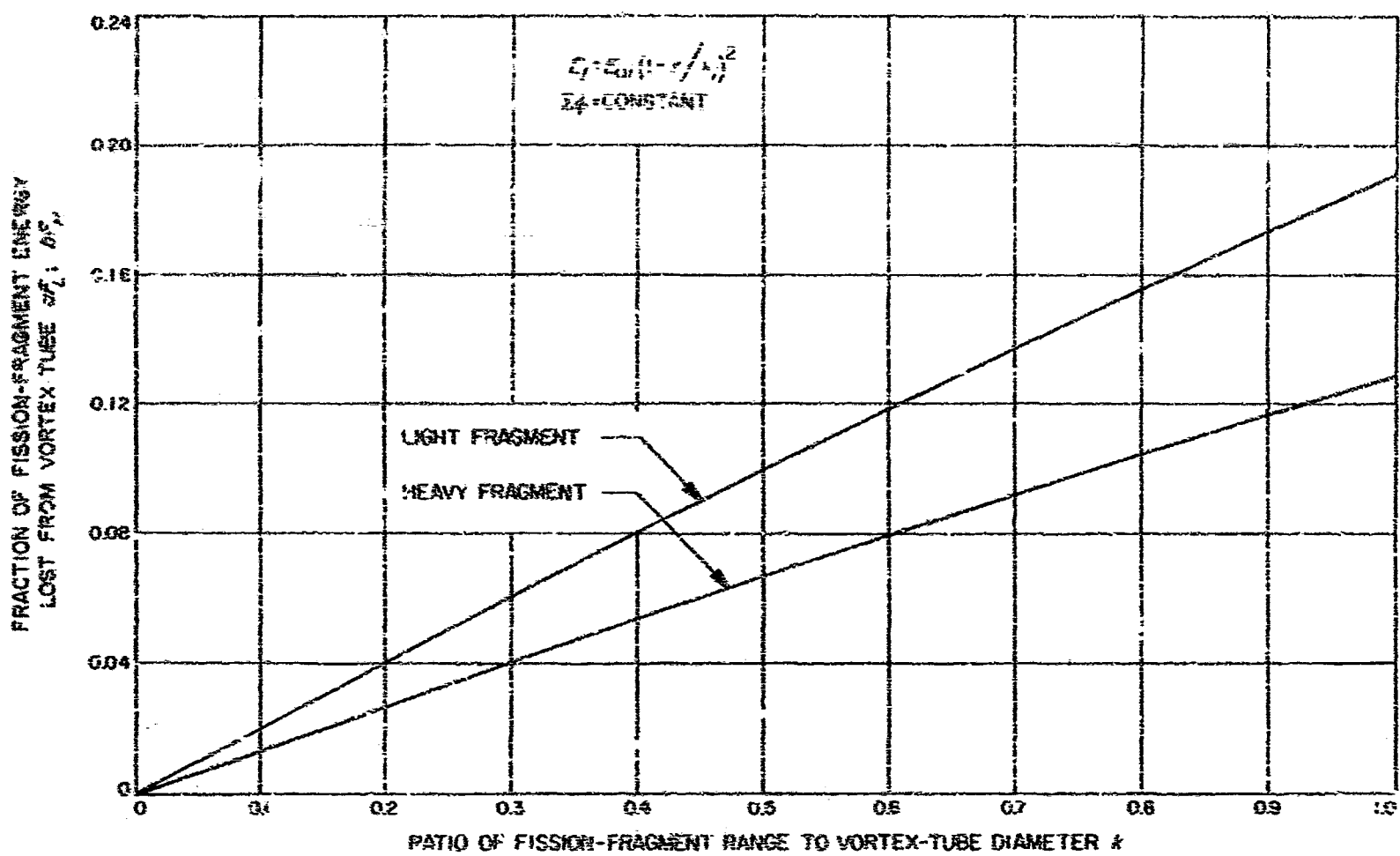


Fig. 5. Fraction of fission-fragment energy lost from vortex tube as a function of k ; linear velocity

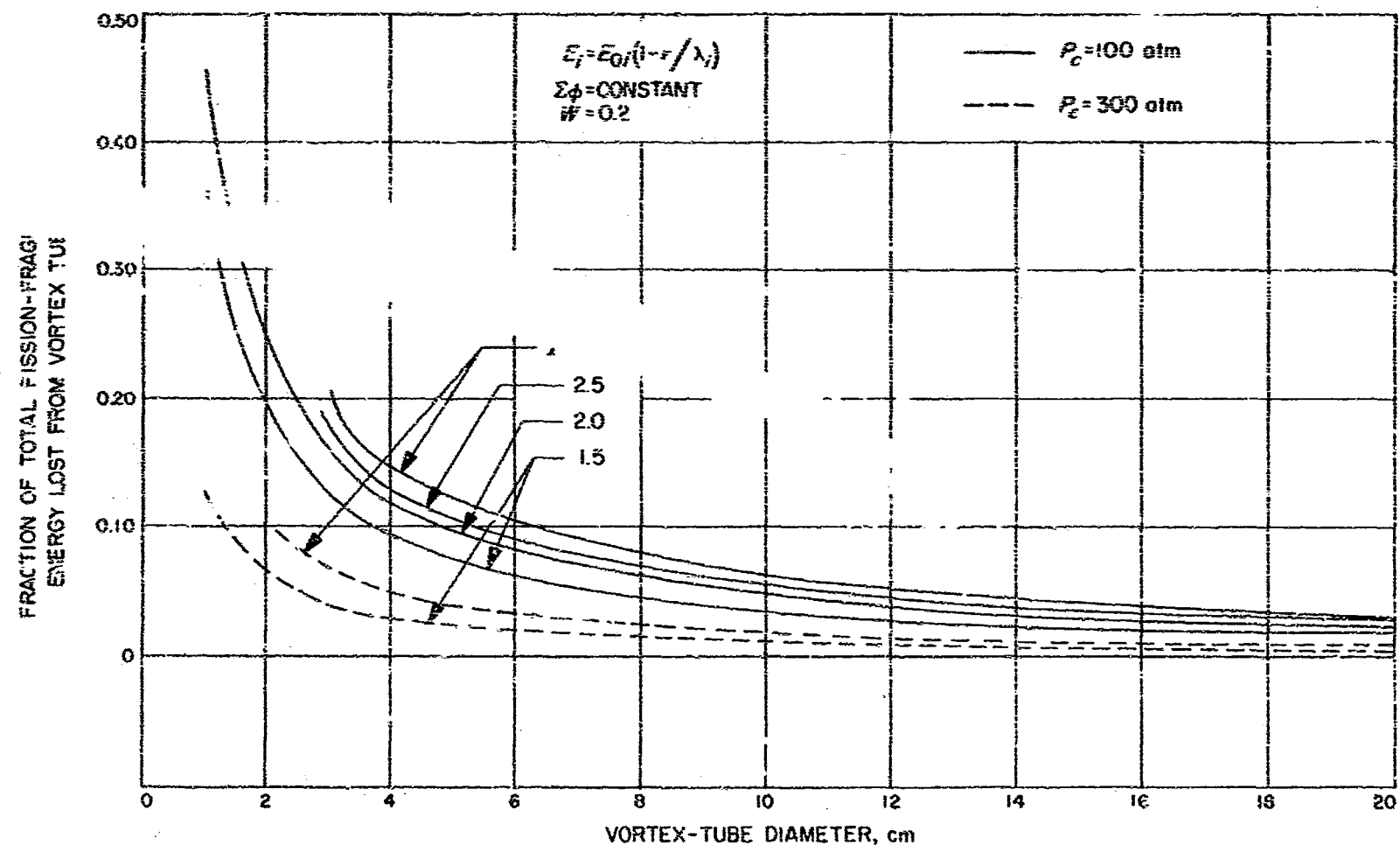


Fig. 6. Fraction of total fission-fragment energy lost from vortex tube as a function of vortex-tube diameter; linear energy, $W = 0.2$

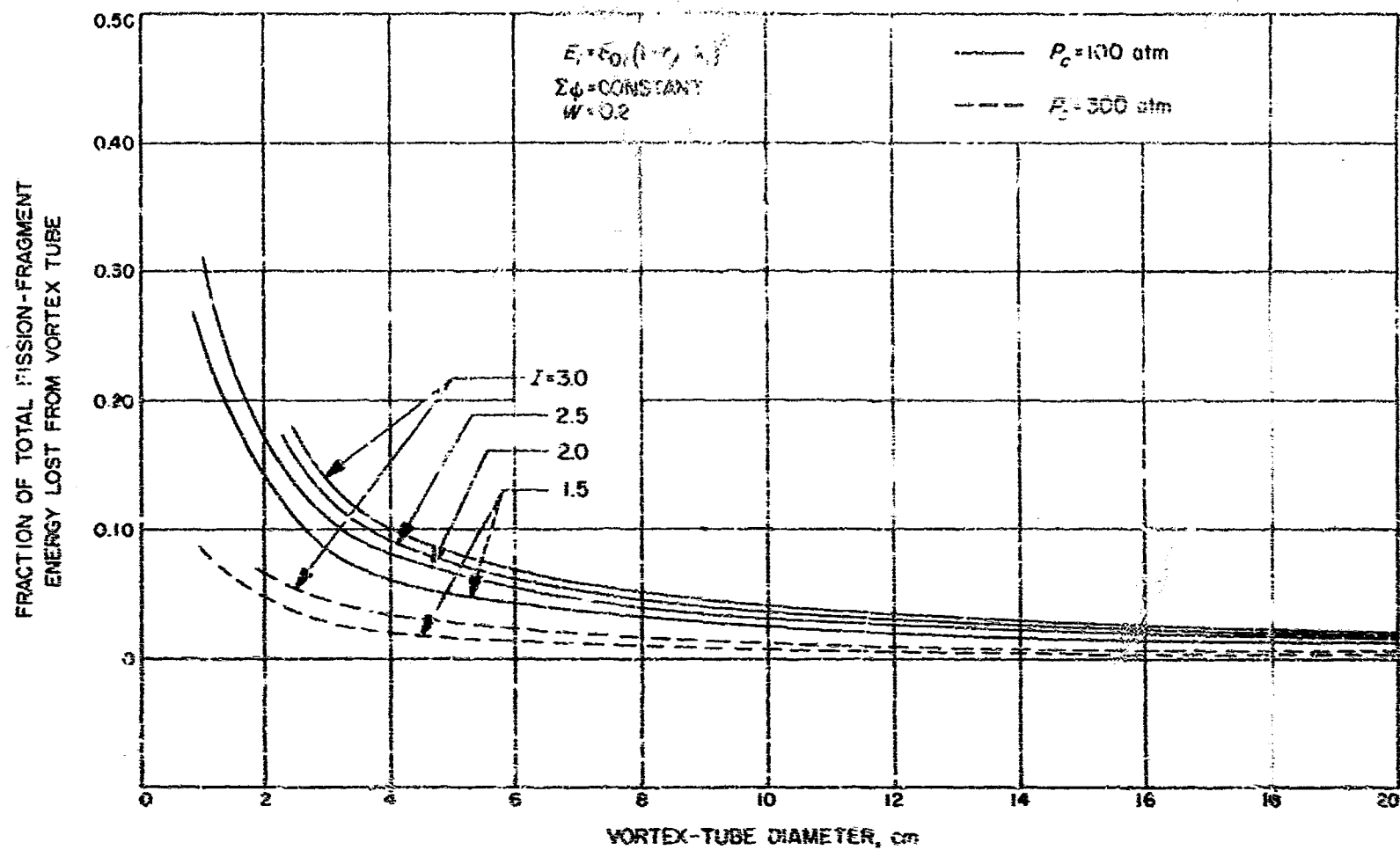


Fig. 7. Fraction of total fission-fragment energy lost from vortex tube as a function of vortex-tube diameter; linear velocity, $W = 0.2$

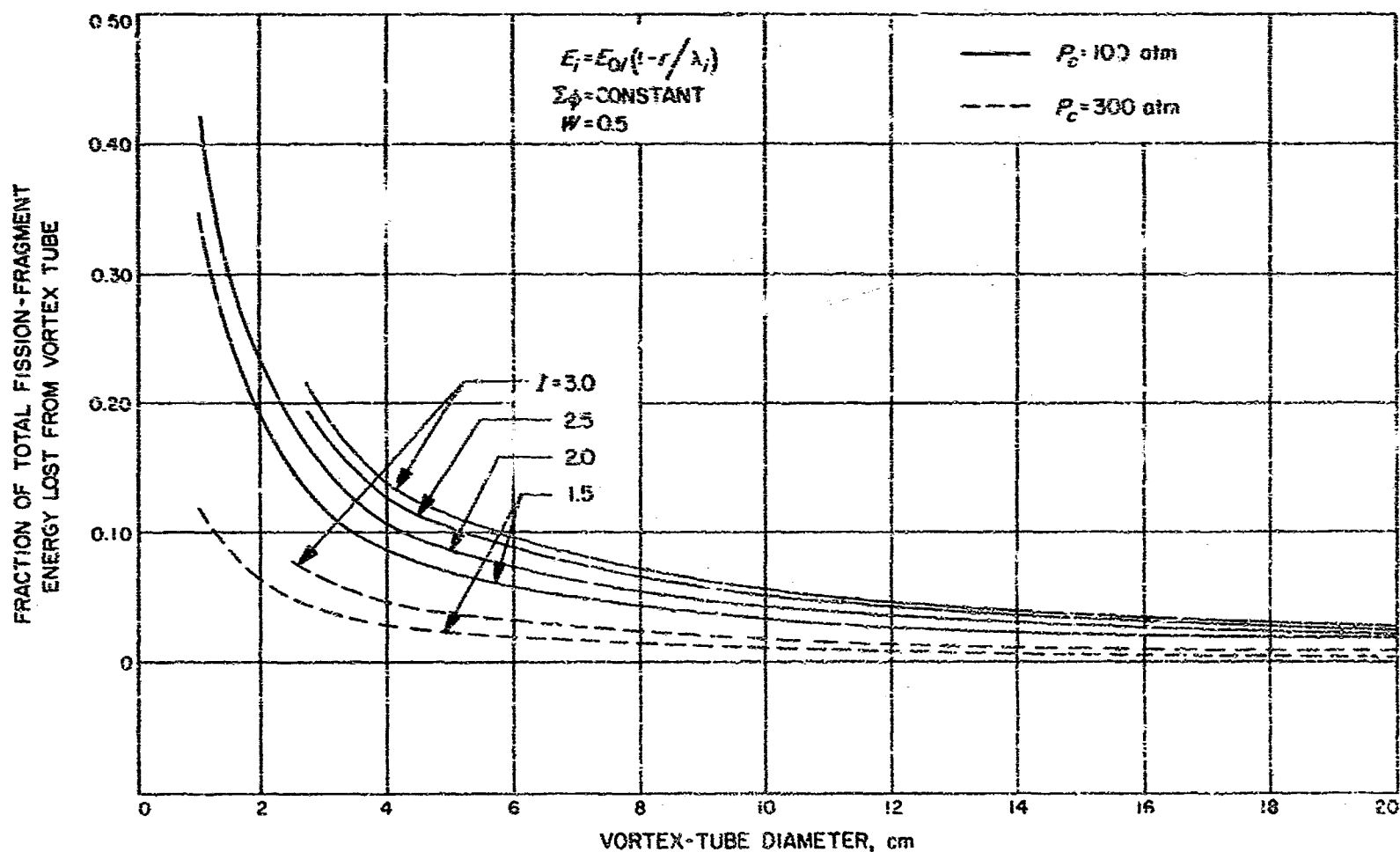


Fig. 8. Fraction of total fission-fragment energy lost from vortex tube as a function of vortex-tube diameter; linear energy, $W = 0.5$

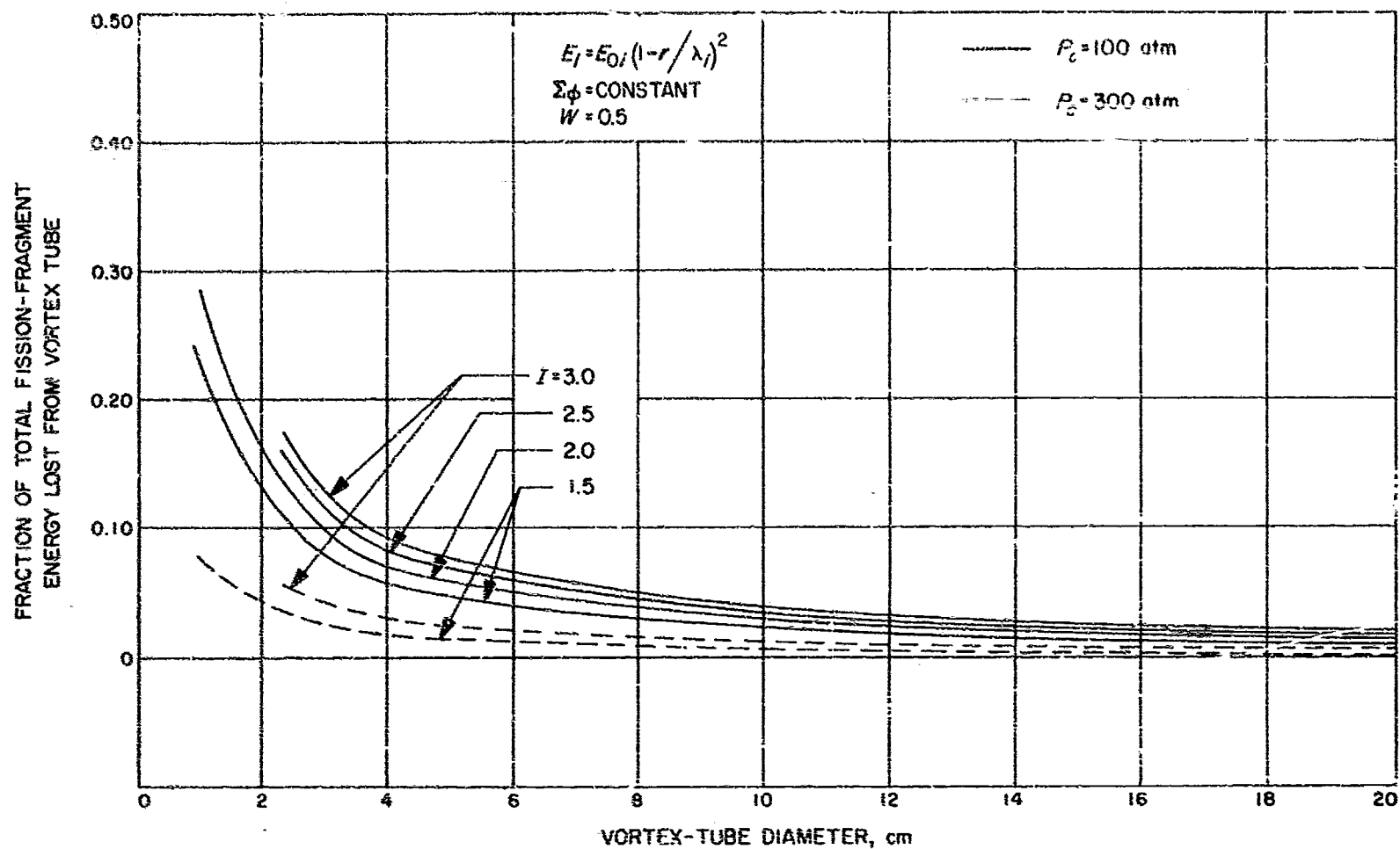


Fig. 9. Fraction of total fission-fragment energy lost from vortex tube as a function of vortex-tube diameter; linear velocity, $W = 0.5$

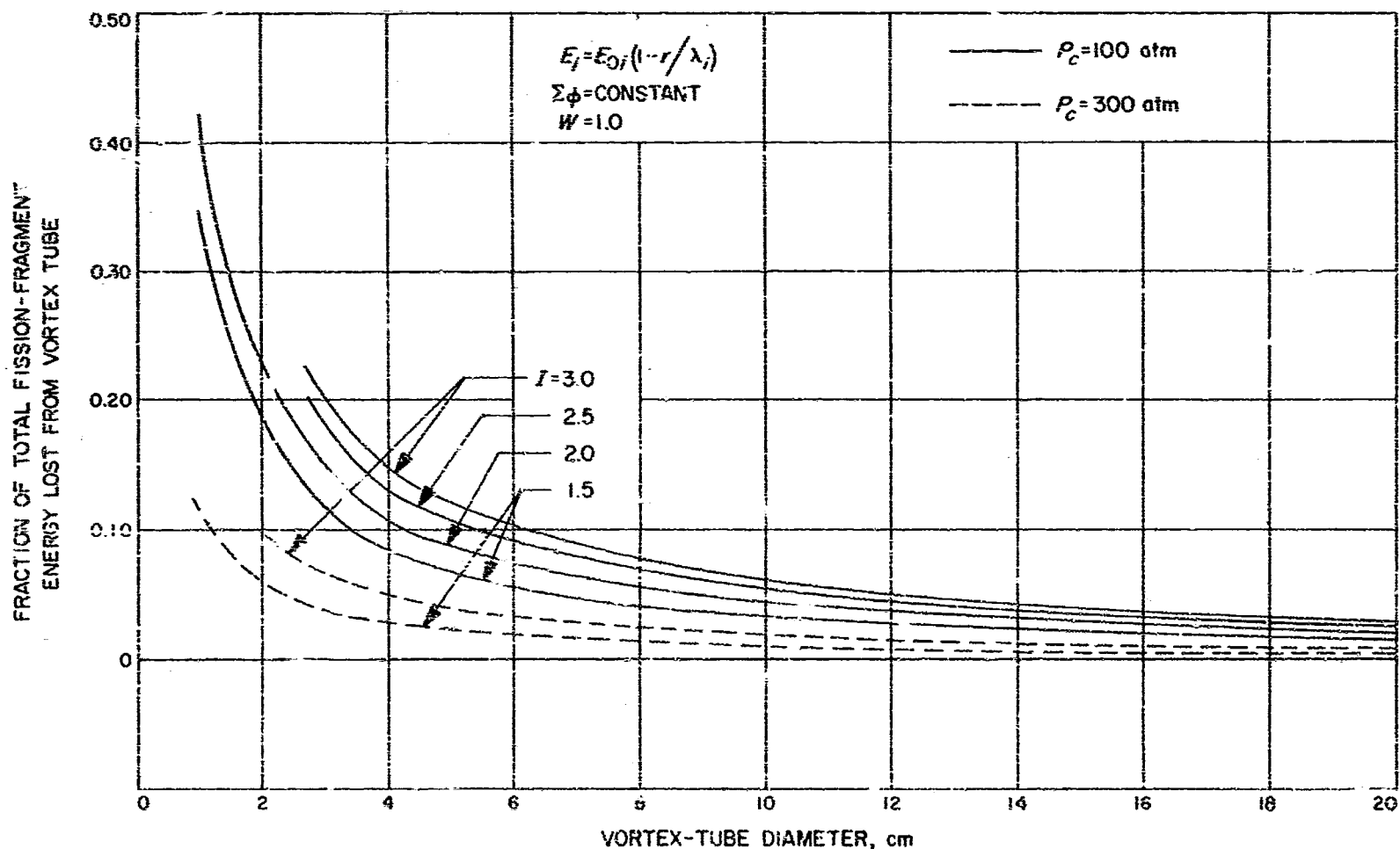


Fig. 10. Fraction of total fission-fragment energy lost from vortex tube as a function of vortex-tube diameter; linear energy, $W = 1.0$

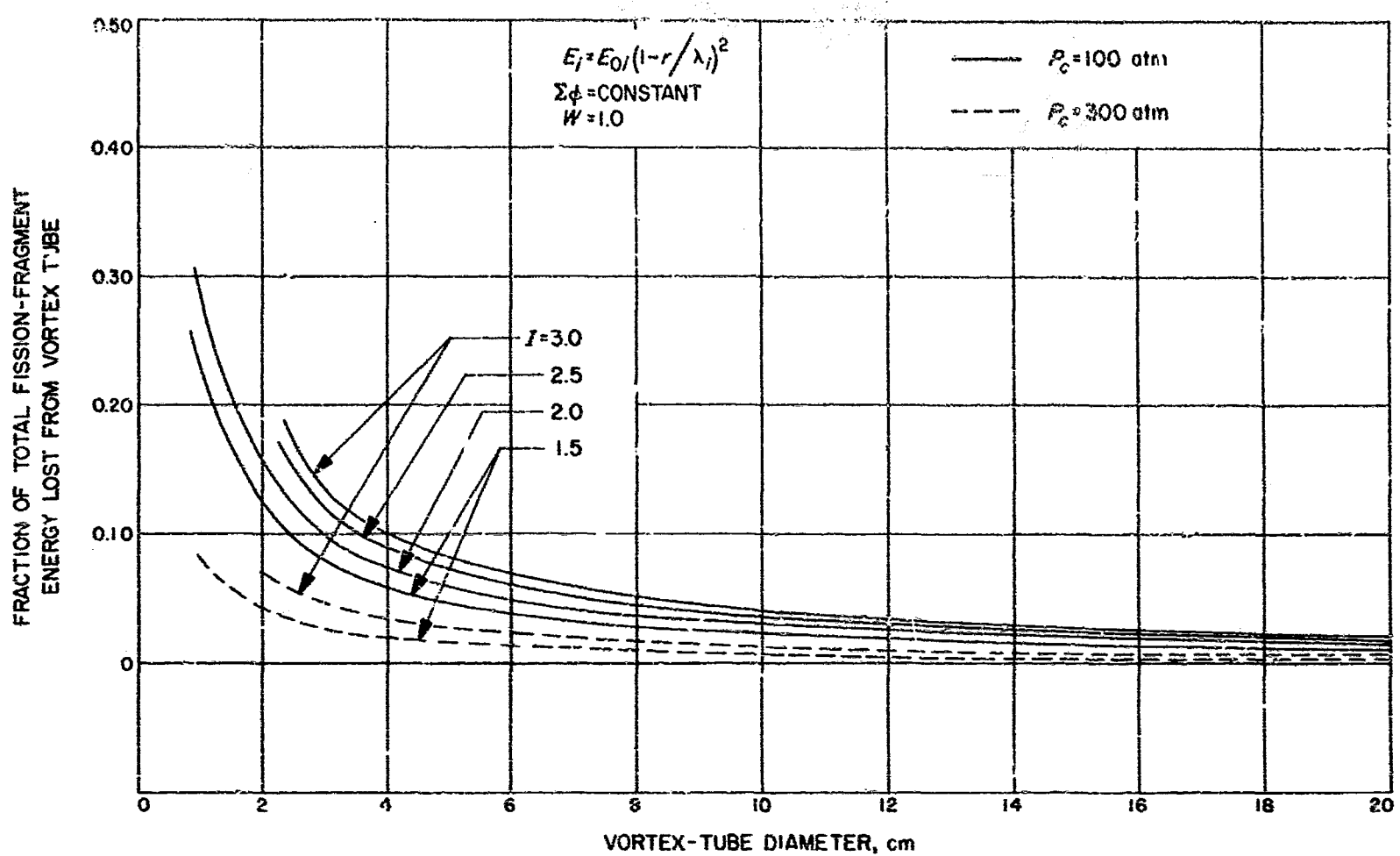


Fig. 11. Fraction of total fission-fragment energy lost from vortex tube as a function of vortex-tube diameter; linear velocity, $W = 1.0$

V. CONCLUSIONS

Within the limits of the present analysis, the following conclusions can be drawn:

1. The heat load in the solid regions of the vortex-tube reactor due to energy deposition by the fission fragments will be only a few percent of the total power if the diameter of the vortex tubes is greater than 20 cm at an exhaust pressure of 100 atm and greater than 8 cm at an exhaust pressure of 300 atm.
2. Increasing the tube diameter beyond these values

will not decrease the fission-fragment heat load significantly.

3. For a fixed set of conditions, the fission-fragment heat load is nearly inversely proportional to the exhaust pressure.
4. For vortex-tube diameters at which the fission-fragment heat load is only a few percent of the total power, the specific-impulse ratio I and the ratio of fuel to propellant density W have little effect on this heat load.

NOMENCLATURE

A	area
a	constant (see Eq. 11)
b	constant (see Eq. 11)
E	energy
$\tilde{E}(\pi/2, \alpha)$	complete elliptic integral of the second kind
F	function defined in Eqs. (16)–(19)
$\tilde{F}(\pi/2, \alpha)$	complete elliptic integral of the first kind
G	function (see Eq. 19)
I	specific-impulse ratio = $\sqrt{T_o/T_p}$
k	ratio of fission-fragment range to vortex-tube diameter
L	length (see Fig. 1)
l	length of vortex tube
P	pressure
Q	function defined by Eq. (6)
R	radius of vortex tube
r	coordinate (see Fig. 1)
S	function (see Eq. 18)
T	temperature
V	volume

W	ratio of fuel density to propellant density
α	arbitrary parameter
β	arbitrary parameter
λ	fission-fragment range
ρ	density
Σ	macroscopic cross-section for fission
τ	fraction of total fission-fragment energy deposited into solid region of reactor
Φ	coordinate (see Fig. 1)
ϕ	thermal-neutron flux
x	coordinate (see Fig. 1)
ψ	coordinate (see Fig. 1)

Subscripts

c	center of vortex tube
h	heavy fission fragment
i	general index
l	light fission fragment
o	initial value
p	periphery of vortex tube
s	standard conditions
t	total energy of fission fragments